

Multi-Scale Factorization of the Wave Equation with Application to Compressed Sensing Photoacoustic Tomography

Gerhard Zangerl and Markus Haltmeier

Department of Mathematics, University of Innsbruck

Technikestraße 13, 6020 Innsbruck, Austria

E-mail: {gerhard.zangerl, markus.haltmeier}@uibk.ac.at

December 15, 2021

Abstract

By performing a large number of spatial measurements, high spatial resolution photoacoustic imaging can be achieved without specific prior information. However, the acquisition of spatial measurements is time consuming, costly and technically challenging. By exploiting non-linear prior information, compressed sensing techniques in combination with sophisticated reconstruction algorithms allow a reduction of number of measurements while maintaining a high spatial resolution. For this purpose, in this paper, we propose a multiscale factorization for the wave equation, which separates the data into a low frequency factor and sparse high frequency factors. By extending the acoustic reciprocal principle, we transfer sparsity in measurements domain to spatial sparsity of the initial pressure, which allows the use of sparse reconstruction techniques. Numerical results are presented which demonstrate the feasibility of the proposed framework.

Keywords: photoacoustic tomography, image reconstruction, limited data, wave equation, cost reduction, compressed sensing, multiscale factorization.

AMS: 45Q05, 65T60, 94A08, 92C55

1 Introduction

Photoacoustic tomography (PAT) is an emerging imaging technique that combines the high resolution of ultrasound imaging with the high contrast of optical tomography [45]. As illustrated in Figure 1, in PAT a semitransparent sample is illuminated by short pulses of optical energy which causes the excitation of an acoustic pressure wave $p: \mathbb{R}^3 \times [0, \infty) \rightarrow \mathbb{R}$, depending the spatial position $x \in \mathbb{R}^3$ and time $t \geq 0$. The initial pressure distribution $f: \mathbb{R}^3 \rightarrow \mathbb{R}$ is proportional

to the inner light absorption properties of the sample and carries valuable diagnostic information. Detectors located on a measurement surface S (partially) surrounding the sample measure the acoustic pressure from which the initial pressure distribution is recovered. Throughout we denote by $\mathbf{W} f := p|_{S \times [0, \infty)}$ the restriction of the acoustic pressure to the measurement surface.

Exact reconstruction formulas are available for complete data for certain surfaces S , see, for example, [12, 14, 16, 21, 32, 33, 37]. Efficient reconstruction schemes in PAT accounting for acoustic attenuation or variable sound speed have also been developed [1, 2, 3, 24, 27, 29, 30, 44]. Different detector types such as linear or circular detectors that record integrals of the acoustic pressure have been investigated [5, 46]. In this paper, we consider the constant sound speed case and address the issue of compressed sensing to reduce the amount of data while maintaining high spatial resolution.

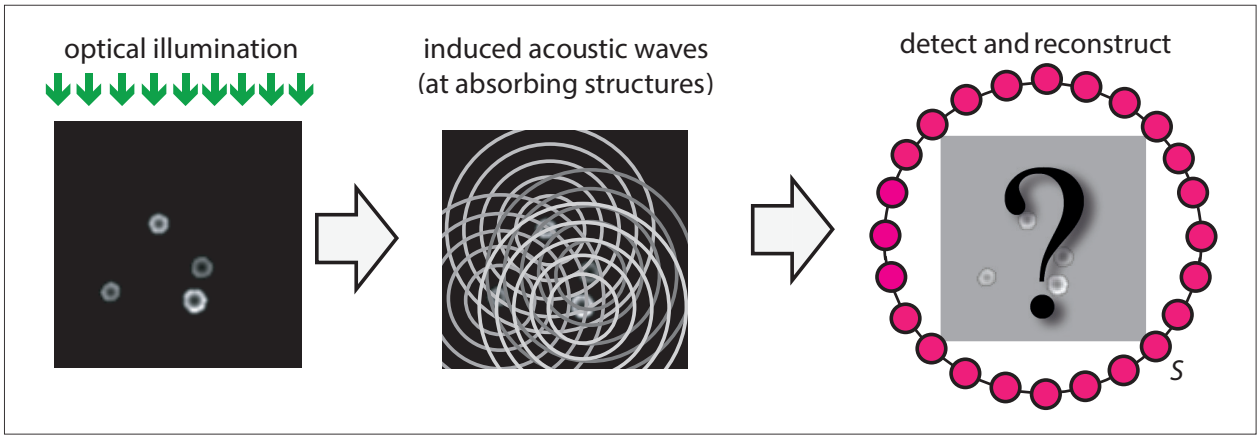


Figure 1: **Basic principles of PAT.** Left: A sample object is illuminated by short optical pulses. Middle: Optical energy is absorbed within the sample, causes non-uniform heating and induces a subsequent acoustic pressure wave. Right: Acoustic sensors located outside of the sample capture the pressure signals, which are used to recover an image of the interior. In this paper, we develop a specific compressed sensing algorithm that allows to reduce the number of spatial measurements while keeping high spatial resolution.

1.1 Compressed sensing PAT

Acoustic signals in PAT offer large bandwidth. Therefore, high spatial resolution can be achieved by using a sufficiently large number of measurements [22] as predicted by Shannon's sampling theorem. In practice, however, collecting a high number of measurements either needs a high number of parallel data acquisition channels or many sequential measurements. This either results in an increase of the cost and technical complexity of the system, or significantly increases measurement time. Several approaches accelerating data collection have been proposed. For example, in [38] a phase contrast method has been developed where a reconstruction of the initial pressure can be obtained from projections of the acoustic pressure that can be collected in short time. In the present work, we use compressed sensing techniques [6, 11, 17, 18] to re-

duce the number of measurements while preserving high spatial resolution. Main challenges in compressed sensing are the developments of sophisticated image formation algorithms. In PAT such CS techniques have been developed [23, 25, 4]. Here, we develop a novel image reconstruction strategy based on a multiscale factorization of the wave equation universally applicable to compressed sensing PAT (CSPAT).

Compressed sensing reconstruction techniques are based on the sparsity of the signals to be reconstructed. In PAT, a possible approach is to express the initial density in a suitable basis. Using such a strategy leads to a coupled forward model that might be numerically challenging to be solved. As an alternative, strategies that apply a transform in the time domain to sparsify PAT data have been proposed in [42, 23]. These methods have been demonstrated to very well reconstruct the high frequency content of the initial pressure from a significantly reduced amount of measurements. However, the proposed differential operators used as sparsifying transforms suppress low frequency information of the acoustic signals which results in low-frequency artefacts in the reconstruction.

1.2 Main Contributions

In this work, we develop the concept multiscale temporal transforms and multiscale factorization for CSPAT. We apply multiscale transforms in the time domain that separate the data into a low frequency component and several high frequency components. The main idea of the proposed reconstruction scheme is to use the acoustic reciprocal principle to show that there is a one-to-one correspondence between the transform data in the time domain and spatially transformed initial pressure. This factorization allows the use of sparse recovery techniques for the high frequency factor of the initial pressure while the low frequency part can be inverted with standard methods. To be more specific, for a mother wavelet function $v: \mathbb{R} \rightarrow \mathbb{R}$ we set $v_j(t) = 2^j \phi(2^j t)$ for $j \geq 1$ and denote by v_0 a function containing missing low frequency content. For example, this might be the associated scaling function of mother wavelet. We then explicitly derive associated functions $u_j: \mathbb{R}^2 \rightarrow \mathbb{R}$ such that for any initial pressure we have the reciprocal relation

$$\mathbf{W}(f \otimes_x u_j) = v_j \otimes_t (\mathbf{W} f) \quad \text{for all } j \in \mathbb{N}. \quad (1)$$

The latter identity is then used in the context of compressed sensing data instead of classical data $\mathbf{W} f$. Based on (1), we develop a reconstruction strategy for recovering a multiscale decomposition of the initial pressure consisting of several sparse high frequency parts and on smooth version of the initial pressure distribution f . Figure (2) shows a phantom f pressure data $\mathbf{W} f$ and the corresponding multiscale factors $v_j \otimes_t (\mathbf{W} f)$ (top) and $f \otimes_x u_j$ (bottom).

The concept of sparsifying temporal transforms for CSPAT has been originally developed for PAT in [42, 23] for two and three spatial dimensions. These earlier approaches use a single scale sparsifying transform. The sparsifying transforms filter out low frequency components which results in low frequency artefacts in the reconstruction. By also considering an additional low

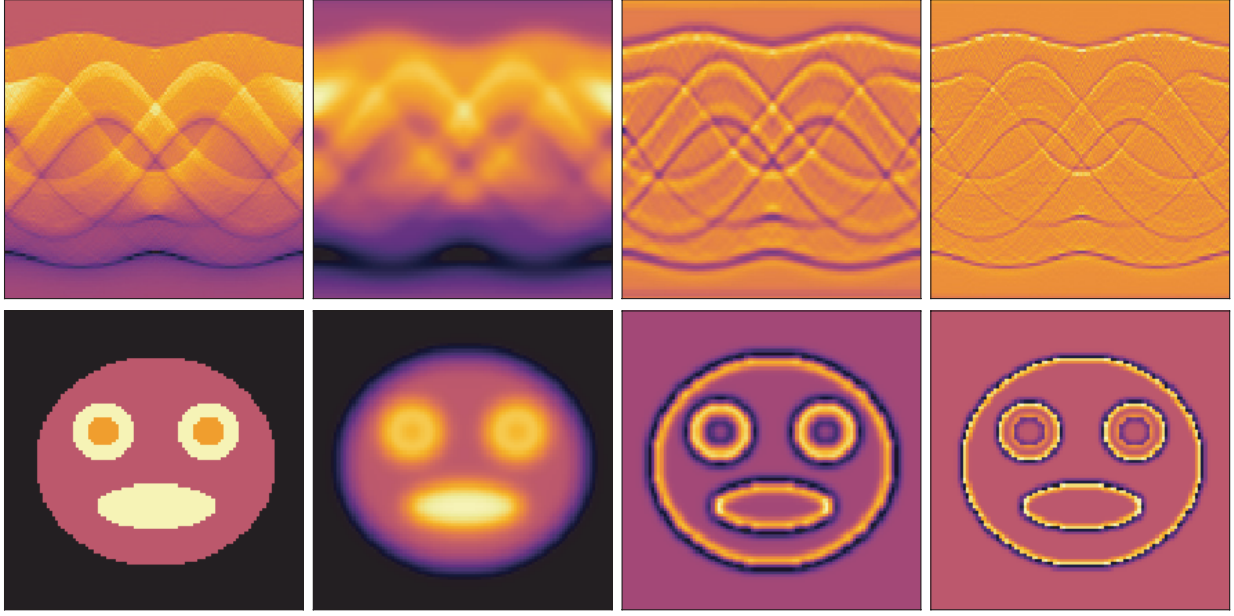


Figure 2: Top: Data $\mathbf{W} f$ (left) and convolved pressure data $v_j \otimes_t \mathbf{W} f$ at three different scales. Bottom: Initial pressure f and convolved initial pressure $f \otimes_x u_j$ as the same scales. According to the acoustic reciprocal principle (1), the convolved pressure data are corresponding to the convolved initial data for which we have sparsity, that we employ for compresses sensing reconstruction.

frequency component, the proposed multiscale scheme naturally overcomes this drawback of single multiscale transforms. Another solution to the missing low frequency content has been proposed in [25] where we proposed to jointly recover the initial pressure f and a sparsified version of f based on second time derivative. However, the present approach seems more natural from and more accessible to rigorous mathematical analysis.

1.3 Outline

The remainder of the paper is organized as follows. In Section 2 we present required background from PAT and derive a dual form acoustic reciprocal principle. In Section 3 we derive a multiscale factorization for the wave equation. The application to CSPAT is presented Section 4. Numerical illustrations are provided in Section 5. The paper end with a short summary and outlook presented in Section 6.

2 Photoacoustic tomography

In this section, we provide the required background from PAT and derive a reciprocal version of the acoustic reciprocal principle that is required for our later analysis.

2.1 Wave equation model

Throughout we consider PAT using constant speed of sound propagation. The acoustic pressure is modeled as a function $p: \mathbb{R}^d \times [0, \infty) \rightarrow \mathbb{R}$ that satisfies the following initial value problem for the wave equation

$$p_{tt}(x, t) - \Delta p(x, t) = 0 \quad \text{for } (x, t) \in \mathbb{R}^d \times (0, \infty), \quad (2)$$

$$p(x, 0) = f(x) \quad \text{for } x \in \mathbb{R}^d, \quad (3)$$

$$p_t(x, 0) = 0 \quad \text{for } x \in \mathbb{R}^d. \quad (4)$$

Here $f \in C^\infty(\mathbb{R}^3)$ is the initial pressure distribution that for simplicity we assume to be smooth. Note that in the practical application the cases $d = 2$ and $d = 3$ are relevant [5, 15, 16, 31, 45].

Continuous PAT data consist of time resolved acoustic pressure restricted in space to a smooth detection surface $S \subseteq \mathbb{R}^3$. The continuous PAT forward operator is given by,

$$\mathbf{W}: C^\infty(\mathbb{R}^3) \rightarrow C^\infty(S \times (0, \infty)): f \mapsto \mathbf{W}f = p|_{S \times (0, \infty)}. \quad (5)$$

The corresponding full data inverse problem consists in solving the operator equation $\mathbf{W}f = g$ from possible noisy information. In the last two decades, many methods including exact reconstruction formulas and iterative methods, for different geometries, variable and constant sound speed and detector types have been developed by researchers, see [40] for a recent review. Clearly, in practice only discrete data can be collected. We will present standard discrete sensing as well as compressed sensing strategies in Section 4.

2.2 Acoustic reciprocal principle

Compressed sensing reconstruction techniques are typically based on sparsity of the unknown signals to be reconstructed. To obtain sparsity in PAT we use the acoustic reciprocal principle in combination with sparsifying temporal transforms. The acoustic reciprocal principle states that manipulating photoacoustic data in the temporal domain corresponds to a spatial convolution of the initial pressure with a radial function. An explicit form of acoustic reciprocal principle was first proven in [26] for three spatial dimensions and extended in [20] for arbitrary dimension.

Proposition 1 (Acoustic reciprocal principle of [20]). *Let $u \in L^1(\mathbb{R}^d)$ be a compactly supported radial function of the form $u = \bar{u}(\|\cdot\|)$ and set*

$$\mathbf{R}u: \mathbb{R} \rightarrow \mathbb{R}: t \mapsto \begin{cases} \bar{u}(t) & \text{if } d = 1 \\ \omega_{d-2} \int_{|t|}^{\infty} \bar{u}(s) (s^2 - t^2)^{(d-3)/2} s ds & \text{if } d > 1, \end{cases} \quad (6)$$

where ω_{d-2} denote the volume of the $(d-2)$ -dimensional unit sphere \mathbb{S}^{d-2} . Then, for every $f \in$

$C^\infty(\mathbb{R}^d)$ we have

$$\forall (x, t) \in \mathbb{R}^d \times (0, \infty): \quad \mathbf{W}(u \otimes_x f)(x, t) = ((\mathbf{R}u) \otimes_t \mathbf{W}f)(x, t). \quad (7)$$

Here \otimes_x denotes the spatial convolution in \mathbb{R}^d and \otimes_t denotes the one-dimensional convolution applied in the second component.

This Lemma serves as the basis for the derived multiscale factorization for the wave equation and the resulting sparse reconstruction strategy. Actually, we use the following dual version where we prescribe the temporal filter v instead of prescribing the spatial filter u .

Proposition 2 (Acoustic reciprocal principle, dual version). *Let $v: \mathbb{R} \rightarrow \mathbb{R}$ be an even function with sufficient decay such that $v \circ \sqrt{|\cdot|} \in C^{\lceil (d-1)/2 \rceil}(\mathbb{R})$ and define*

$$\mathbf{R}^\sharp v: \mathbb{R}^d \rightarrow \mathbb{R}: x \mapsto \begin{cases} \frac{(-1)^{(d-1)/2}}{\sqrt{\pi^{d-1}}} \left(\left(\frac{1}{2t} \frac{\partial}{\partial t} \right)^{(d-1)/2} v \right)(\|x\|) & \text{for } d \text{ odd} \\ \frac{2(-1)^{(d-2)/2}}{\sqrt{\pi^d}} \int_{\|x\|}^\infty \frac{\left(\frac{1}{2t} \frac{\partial}{\partial t} \right)^{d/2} v(t)}{\sqrt{t^2 - \|x\|^2}} t dt & \text{for } d \text{ even.} \end{cases} \quad (8)$$

Then, for every $f \in C^\infty(\mathbb{R}^d)$,

$$\forall (x, t) \in \mathbb{R}^d \times (0, \infty): \quad v \otimes_t (\mathbf{W}f)(x, t) = \mathbf{W} \left((\mathbf{R}^\sharp v) \otimes_x f \right)(x, t). \quad (9)$$

Proof. The proof is given in Appendix A. □

Note that the assumption $v \circ \sqrt{|\cdot|} \in C^{\lceil (d-1)/2 \rceil}(\mathbb{R})$ is made such that the derivatives in (8) are well-defined in the classical sense.

3 Multiscale factorizations of the wave equation

Based on the acoustic reciprocal principle, in this section we derive convolution factorization for PAT. For that purpose, we first recall some results for convolutional frames. Then we introduce convolutional frame decompositions in Subsection 3.2, which are used to derive multiscale factorizations in Subsection 3.3.

3.1 Convolutional frames

Let Λ be an at most countable index set and consider a family $(u_\lambda)_{\lambda \in \Lambda}$ of functions in $L^2(\mathbb{R}^d) \cap L^1(\mathbb{R}^d)$. According to the convolution theorem we have $f \otimes_x u_\lambda = \mathbf{F}_d^{-1}((\mathbf{F}_d f) \cdot (\mathbf{F}_d u_\lambda))$ for all $f \in L^2(\mathbb{R}^d)$. Moreover, $f \otimes_x u_\lambda$ is well defined almost everywhere and satisfies $f \otimes_x u_\lambda \in L^2(\mathbb{R}^d)$. Here and in the following we denote by $\mathbf{F}_d f(\xi) := \int_{\mathbb{R}^d} f(x) e^{-ix \cdot \xi} dx$ for $\xi \in \mathbb{R}^d$ the d -dimensional Fourier transform and \mathbf{F}_d^{-1} its inverse. We write $u^*(x) := u(-x)$ for $u \in L^2(\mathbb{R}^d)$ and note that $\mathbf{F}_d u^* = \overline{[\mathbf{F}_d u]}$, where $[\cdot]$ denotes complex conjugation.

Definition 3 (Convolutional frame). We call a family $\mathbf{u} = (u_\lambda)_{\lambda \in \Lambda} \subseteq (L^2(\mathbb{R}^d) \cap L^1(\mathbb{R}^d))^\Lambda$ a convolutional frame in \mathbb{R}^d , if there are constants $A, B > 0$ such that

$$f \in L^2(\mathbb{R}^d): \quad A \|f\|_2^2 \leq \sum_{\lambda \in \Lambda} \|f \otimes_x u_\lambda\|_2^2 \leq B \|f\|_2^2. \quad (10)$$

If \mathbf{u} is a convolutional frame, we name A, B the frame bounds and call

- (a) $\mathbf{T}_\mathbf{u}: L^2(\mathbb{R}^d) \rightarrow \ell^2(\Lambda, L^2(\mathbb{R}^d))$: $f \mapsto (u_\lambda \otimes_x f)_{\lambda \in \Lambda}$ analysis operator,
- (b) $\mathbf{T}_\mathbf{u}^*: \ell^2(\Lambda, L^2(\mathbb{R}^d)) \rightarrow L^2(\mathbb{R}^d)$: $(f_\lambda)_{\lambda \in \Lambda} \mapsto \sum_{\lambda \in \Lambda} u_\lambda^* \otimes_x f_\lambda$ synthesis operator,
- (c) $\mathbf{T}_\mathbf{u}^* \mathbf{T}_\mathbf{u}: L^2(\mathbb{R}^d) \rightarrow L^2(\mathbb{R}^d)$: $f \mapsto \sum_{\lambda \in \Lambda} u_\lambda^* \otimes_x u_\lambda \otimes_x f$ frame operator.

Finally, we call \mathbf{u} tight if $\mathbf{T}_\mathbf{u}^* \mathbf{T}_\mathbf{u} = \mathbf{I}$.

Note that $\ell^2(\Lambda, L^2(\mathbb{R}^d))$ is a Hilbert space with inner product $\langle \mathbf{a}, \mathbf{b} \rangle_\Lambda := \sum_{\lambda \in \Lambda} \langle a_\lambda, b_\lambda \rangle$ and corresponding norm $\|\cdot\|_\Lambda$. Using the analysis operator, we can write the defining identity (10) in the form $A \|f\|_2^2 \leq \|\mathbf{T}_\mathbf{u} f\|_\Lambda^2 \leq B \|f\|_2^2$. Hence the right inequality states that $\mathbf{T}_\mathbf{u}: L^2(\mathbb{R}^d) \rightarrow \ell^2(\Lambda, L^2(\mathbb{R}^d))$ is well defined and bounded, whereas the left inequality states that $\mathbf{T}_\mathbf{u}$ has a bounded Moore-Penrose inverse $\mathbf{T}_\mathbf{u}^+: \ell^2(\Lambda, L^2(\mathbb{R}^d)) \rightarrow L^2(\mathbb{R}^d)$. Further note that $\mathbf{T}_\mathbf{u}^*$ is the adjoint of $\mathbf{T}_\mathbf{u}$.

Lemma 4 (Characterization of convolutional frames). *For any family $\mathbf{u} = (u_\lambda)_{\lambda \in \Lambda}$ of functions in $L^2(\mathbb{R}^d) \cap L^1(\mathbb{R}^d)$, the following statements are equivalent:*

- (i) \mathbf{u} is a convolutional frame with frame bounds A, B .
- (ii) The identity $A \leq \sum_{\lambda \in \Lambda} |\mathbf{F}_d u_\lambda|^2 \leq B$ holds almost everywhere.

Proof. The convolution theorem and the isometry property of Fourier transform imply that (10) holds if and only if for all $f \in L^2(\mathbb{R}^d)$ we have

$$A \int_{\mathbb{R}^d} |\mathbf{F}_d f(\xi)|^2 d\xi \leq \int_{\mathbb{R}^d} |\mathbf{F}_d f(\xi)|^2 \sum_{\lambda \in \Lambda} |\mathbf{F}_d u_\lambda(\xi)|^2 d\xi \leq B \int_{\mathbb{R}^d} |\mathbf{F}_d f(\xi)|^2 d\xi.$$

This is in turn equivalent that Item (ii) holds. □

In particular, \mathbf{u} is tight if and only if $\sum_{\lambda \in \Lambda} |\mathbf{F}_d u_\lambda|^2 = 1$ almost everywhere.

Lemma 5 (and definition of a dual convolutional frame). *Let $\mathbf{u} = (u_\lambda)_{\lambda \in \Lambda}$ and $\mathbf{w} = (w_\lambda)_{\lambda \in \Lambda}$ be two convolutional frames in \mathbb{R}^d . Then the following statements are equivalent:*

- (i) The identity $\sum_{\lambda \in \Lambda} \overline{[\mathbf{F}_d w_\lambda]} \cdot (\mathbf{F}_d u_\lambda) = 1$ holds almost everywhere.
- (ii) The reproducing formula $\forall f \in L^2(\mathbb{R}^d)$: $\mathbf{T}_\mathbf{w}^* \mathbf{T}_\mathbf{u} f = \sum_{\lambda \in \Lambda} w_\lambda^* \otimes_x (u_\lambda \otimes_x f) = f$ holds.

If (i), (ii) hold, we call $(w_\lambda)_{\lambda \in \Lambda}$ a dual convolutional frame of $(u_\lambda)_{\lambda \in \Lambda}$.

Proof. The linearity and continuity of the Fourier transform together with the convolution theorem show that the identity in (ii) is equivalent to the identity $(\mathbf{F}_d f) \cdot \sum_{\lambda \in \Lambda} (\mathbf{F}_d w_\lambda^*) \cdot (\mathbf{F}_d u_\lambda) = \mathbf{F}_d f$ for all $f \in L^2(\mathbb{R}^d)$. Because $\mathbf{F}_d w_\lambda^* = \overline{(\mathbf{F}_d w_\lambda)}$ this implies the desired equivalence. \square

In particular, Item (i) in Lemma 5 is satisfied with w taken as the canonical dual convolutional frame $\mathbf{u}^+ := (u_\lambda^+)_{\lambda \in \Lambda}$ defined by

$$\forall \mu \in \Lambda: \quad \mathbf{F}_d u_\mu^+ := \frac{\mathbf{F}_d u_\mu}{\sum_{\lambda \in \Lambda} |\mathbf{F}_d u_\lambda|^2}. \quad (11)$$

In this case we have $\mathbf{T}_{\mathbf{u}^+} = \mathbf{T}_{\mathbf{u}}^+$, where $\mathbf{T}_{\mathbf{u}}^+$ denotes the Moore-Penrose inverse of the analysis operator $\mathbf{T}_{\mathbf{u}}$.

3.2 Convolution factorization

The following concept is central for this paper.

Definition 6 (Convolution factorization of the wave equation). Let Λ be an at most countable index set and consider families $\mathbf{u} = (u_\lambda)_{\lambda \in \Lambda} \in (L^2(\mathbb{R}^d))^\Lambda$ and $\mathbf{v} = (v_\lambda)_{\lambda \in \Lambda} \in (L^2(\mathbb{R}))^\Lambda$. We call the pair (\mathbf{u}, \mathbf{v}) a convolution factorization for \mathbf{W} if the following hold:

(CFD1) $(u_\lambda)_{\lambda \in \Lambda}$ is a convolutional frame of $L^2(\mathbb{R}^d)$,

(CFD2) $(v_\lambda)_{\lambda \in \Lambda}$ is a convolutional frame of $L^2(\mathbb{R})$,

(CFD3) The commutation relation holds $\forall f \in L^2(K)$: $\mathbf{W}(u_\lambda \otimes_x f) = v_\lambda \otimes_t (\mathbf{W} f)$.

Given a convolution factorization (\mathbf{u}, \mathbf{v}) for \mathbf{W} and data $g = \mathbf{W} f$ the commutation relation (CFD3) formula shows that is sufficient to solve each equation $\mathbf{W} f_\lambda = v_\lambda \otimes_t g$. These equations now involve the unknown $f_\lambda = u_\lambda \otimes_x f$ having specific prior information, that we can exploited for inversion. Moreover, we will later show that the same identity holds for any spatial sampling scheme, enabling it for CSPAT. It is well known that \mathbf{W} is injective when restricted to function having some decay. Therefore, if (\mathbf{u}, \mathbf{v}) is a convolution factorization and $u_\lambda \otimes_x f$ has sufficient decay we have the reproducing formula

$$f = \sum_{\lambda \in \Lambda} u_\lambda^* \otimes_x \mathbf{W}^{-1}(v_\lambda \otimes_t (\mathbf{W} f)) \quad (12)$$

In fact, the factorization identity (12) is the reason why we name a pair (\mathbf{u}, \mathbf{v}) satisfying (CFD1)-(CFD3) a convolution factorization.

As the main theoretical result, in this paper we construct explicit convolution factorizations for

the PAT forward operator. For that purpose, recall

$$\mathbf{R}^\# v: \mathbb{R}^d \rightarrow \mathbb{R}: x \mapsto \begin{cases} \frac{(-1)^{(d-1)/2}}{\sqrt{\pi^{d-1}}} \left(\left(\frac{1}{2t} \frac{\partial}{\partial t} \right)^{(d-1)/2} v \right)(\|x\|) & \text{for } d \text{ odd} \\ \frac{2(-1)^{(d-2)/2}}{\sqrt{\pi^d}} \int_{\|x\|}^{\infty} \frac{\left(\frac{1}{2t} \frac{\partial}{\partial t} \right)^{d/2} v(t)}{\sqrt{t^2 - \|x\|^2}} t dt & \text{for } d \text{ even,} \end{cases}$$

and the dual version of the acoustical reciprocal principle $v \otimes_t (\mathbf{W} f) = \mathbf{W} ((\mathbf{R}^\# v) \otimes_x f)$ stated in Proposition 2.

Theorem 7 (Construction of convolution factorization of the wave equation). *Let $(v_\lambda)_{\lambda \in \Lambda} \in L^2(\mathbb{R})^\Lambda$ be a convolutional frame consisting of even functions v_λ with sufficient decay such that $v_\lambda \circ \sqrt{|\cdot|} \in C^\lceil (d-1)/2 \rceil(\mathbb{R})$ and let $(v_\lambda^*)_{\lambda \in \Lambda}$ be its canonical dual and set $u_\lambda = \mathbf{R}^\# v_\lambda$.*

(a) *The pair $((u_\lambda)_{\lambda \in \Lambda}, (v_\lambda)_{\lambda \in \Lambda})$ is a convolutional frame decomposition for \mathbf{W} .*

(b) *The canonical dual of $(u_\lambda)_{\lambda \in \Lambda}$ is given by $(\mathbf{R}^\# v_\lambda^*)_{\lambda \in \Lambda}$.*

(c) *For all $f \in L^2(\mathbb{R}^d)$, the factors $f_\lambda = u_\lambda \otimes_x f$ satisfy*

$$f = \sum_{\lambda \in \Lambda} u_\lambda^* * f_\lambda, \quad (13)$$

$$\mathbf{W} f_\lambda = v_\lambda \otimes_t \mathbf{W} f. \quad (14)$$

Hence any function $f \in L^2(\mathbb{R}^d)$ can be recovered from data $\mathbf{W} f$ by first solving equation (14) for f_λ and the evaluating the series (13).

Proof. To show Item (a) we verify (CFD1)-(CFD3) from Definition 6. Item (CFD1) is satisfied because $(v_\lambda)_{\lambda \in \Lambda} \in L^2(\mathbb{R})^\Lambda$ is a convolutional frame according to the made assumptions. Item (CFD3) follows from the acoustic reciprocal principle Proposition 1. It remains to verify Item (CFD2), namely that the family $(u_\lambda)_{\lambda \in \Lambda} \in L^2(\mathbb{R})^\Lambda$ is a convolutional frame. For that purpose, recall that $\mathbf{R} \mathbf{R}^\# v_\lambda = v_\lambda$ where \mathbf{R} denotes the Radon transform of a radial function. According to the Fourier slice theorem we have $\mathbf{F}_d \mathbf{R}^\# v_\lambda = \mathbf{F}_1 v_\lambda$. Therefore $\sum_{\lambda \in \Lambda} |\mathbf{F}_d \mathbf{R}^\# v_\lambda|^2 = \sum_{\lambda \in \Lambda} |\mathbf{F}_1 v_\lambda|^2$ which implies that $(\mathbf{R}^\# v_\lambda)_{\lambda \in \Lambda}$ is a convolutional frame according to Lemma 4. Moreover, we have $\mathbf{F}_1 v_\lambda^* = \mathbf{F}_1 v_\lambda / \sum_{\lambda \in \Lambda} |\mathbf{F}_1 v_\lambda|^2$ and therefore

$$\mathbf{F}_1 \mathbf{R}^\# v_\lambda^* = \mathbf{F}_1 v_\lambda^* = \frac{\mathbf{F}_1 v_\lambda}{\sum_{\lambda \in \Lambda} |\mathbf{F}_1 v_\lambda|^2} = \frac{\mathbf{F}_1 \mathbf{R}^\# v_\lambda}{\sum_{\lambda \in \Lambda} |\mathbf{F}_d \mathbf{R}^\# v_\lambda|^2},$$

which shows that $(\mathbf{R}^\# v_\lambda^*)_{\lambda \in \Lambda}$ is the canonical dual of $(\mathbf{R}^\# v_\lambda)_{\lambda \in \Lambda}$ which is Item (b). Finally, Item (c) follows Items (a), (b) and the definitions of a CDF and a dual frame. \square

3.3 Multiscale factorization

As shown in the previous subsection, a convolution factorization splits the image reconstruction into several reconstruction problems, one for each convolved initial data $u_\lambda \otimes_x f$. The basic idea

is now to take $(u_\lambda)_{\lambda \in \Lambda}$ as a multiscale system in order to be able bring sparsity into account.

For given $u \in L^2(\mathbb{R}^d) \cap L^1(\mathbb{R}^d)$ consider the scaled versions

$$u_j: \mathbb{R}^d \rightarrow \mathbb{R}: x \mapsto 2^{jd} u(2^j x) \quad \text{for } j \geq 1. \quad (15)$$

According to the scaling property of the Fourier transform we have $\mathbf{F}_d u_j(\xi) = \mathbf{F}_d u(2^{-j}\xi)$. Suppose that $\mathbf{F}_d u$ is essentially supported $\{\xi \in \mathbb{R}^d \mid b_0 \leq \|\xi\| < 2b_0\}$. Then, as j increases the Fourier transform $\mathbf{F}_d u_j$ are essentially supported in $\{\xi \in \mathbb{R}^d \mid 2^{j-1}b_0 < \|\xi\| \leq 2^j b_0\}$. Its union covers all frequencies except the low frequencies that are contained in the ball $B_0 = \{\xi \in \mathbb{R}^d \mid \|\xi\| < b_0\}$. In order to obtain a convolutional frame with reasonable constants we therefore select another function $u_0 \in L^2(\mathbb{R}^d)$ such that $\mathbf{F}_d u_0$ covers frequencies in b_0 .

Definition 8 (Multiscale convolution decomposition). Let $u_0, u \in L^2(\mathbb{R}^d) \cap L^1(\mathbb{R}^d)$ and define u_j for $j \geq 1$ by (15). We call the family $(u_j)_{j \in \mathbb{N}}$ a multiscale convolution decomposition in $L^2(\mathbb{R}^d)$ if it forms a convolutional frame. For $f \in L^2(\mathbb{R}^d)$, we refer to $f \otimes_x u_0$ as the low frequency factor and to $f * u_j$ for $j \geq 1$ as the high frequency factor at scale j .

According to Lemma 4 and the scaling property of the Fourier transform, the family $\mathbf{u} = (u_j)_{j \in \mathbb{N}}$ is a multiscale decomposition if and only if there are constants $A, B > 0$ such that

$$A \leq \sum_{j \in \mathbb{N}} |\mathbf{F}_d u_j(\xi)|^2 \leq B \quad \text{for almost every } \xi \in \mathbb{R}^d. \quad (16)$$

Moreover, the canonical dual frame $\mathbf{u}^* = (u_j^*)_{j \in \mathbb{N}}$ of \mathbf{u} is given by the Fourier representation $\mathbf{F}_d u_j^* := \mathbf{F}_d u_j / \sum_{k \in \mathbb{N}} |\mathbf{F}_d u_k|^2$ for $j \in \mathbb{N}$. In the one-dimensional case we write $(v_j)_{j \in \mathbb{N}}$ for a multiscale decomposition.

Definition 9 (Multiscale factorization of the wave equation). We call a pair (\mathbf{u}, \mathbf{v}) a multiscale factorization of \mathbf{W} if it is a convolutional frame decomposition such that $\mathbf{u} = (u_j)_{j \in \mathbb{N}}$ and $\mathbf{v} = (v_j)_{j \in \mathbb{N}}$ are multiscale decompositions in $L^2(\mathbb{R}^d)$ and $L^2(\mathbb{R})$, respectively.

From Theorem 7 we immediately get the following.

Theorem 10 (Construction of multiscale factorization of the wave equation). Let $\mathbf{v} = (v_j)_{j \in \mathbb{N}}$ be a multiscale decomposition in $L^2(\mathbb{R})$ consisting of even functions with sufficient decay, let \mathbf{v}^* be its canonical dual and define $\mathbf{u} = (\mathbf{R}^\# v_j)_{j \in \mathbb{N}}$. Then the following holds

- (a) The pair (\mathbf{u}, \mathbf{v}) is a multiscale factorization for \mathbf{W} .
- (b) The canonical dual $(u_j^*)_{j \in \mathbb{N}}$ of \mathbf{u} has the Fourier representation

$$\mathbf{F}_d u_j^*(\xi) = \frac{1}{\sum_{j \in \mathbb{N}} |\mathbf{F}_1 v_j(\|\xi\|)|^2} \mathbf{F}_1 v_j(\|\xi\|). \quad (17)$$

(c) For all $f \in L^2(\mathbb{R}^d)$ the factors $f_j := u_j \otimes_x f$ satisfy

$$f = \sum_{j \in \mathbb{N}} u_j^* \otimes_x f_j \quad (18)$$

$$\mathbf{W} f_j = v_j \otimes_t \mathbf{W} f. \quad (19)$$

Hence any $f \in L^2(\mathbb{R}^d)$ can be recovered from $\mathbf{W} f$ by first solving (19) and then evaluating the series (18).

Proof. Follows from Theorem 7. □

Alternatively, we have the following result that avoids computing the canonical dual.

Corollary 11 (Multiscale reconstruction for the wave equation). *Let $(v_j)_{j \in \mathbb{N}} \in (L^2(\mathbb{R}))^{\mathbb{N}}$ be a multiscale decomposition consisting of even functions v_j with sufficient decay such that $v_j \circ \sqrt{|\cdot|} \in C^{\lceil (d-1)/2 \rceil}(\mathbb{R})$ and set $u_j = \mathbf{R}^\sharp v_j$. Then, all $f \in L^2(\mathbb{R}^d)$ the factors $f_j = u_j \otimes_x f$ satisfy*

$$\Phi \otimes_x f = \sum_{j \in \mathbb{N}} u_j \otimes_x f_j \quad (20)$$

$$\mathbf{W} f_j = v_j \otimes_t \mathbf{W} f, \quad (21)$$

with $\Phi := \mathbf{F}_d^{-1} \left(\sum_{j \in \mathbb{N}} |\mathbf{F}_d u_j|^2 \right)$.

Proof. Similar to the proof of Theorem 7. □

From Corollary 11 it follows that any function $f \in L^2(\mathbb{R}^d)$ can be recovered from data $\mathbf{W} f$ by means of the following consecutive steps

- Solve equation (21) for f_j
- Evaluate the series on the right hand side of (20)
- Solve the deconvolution problem (20) for f .

Because the $(v_\lambda)_{\lambda \in \Lambda}$ is a convolutional frame, $\mathbf{F}_d \Phi$ is bounded away from zero and therefore the deconvolution problem (20) is stably solvable. Because inversion of the wave equation in the full data case is stable, also (21) can be stably solved for f_j . In the case of compressed sensing this will not be the case and we will have to include additional prior information for its solution.

Remark 12 (Examples for multiscale decompositions). Possible multiscale decompositions can be constructed via a dyadic translation invariant wavelet frame, which names a convolutional frame $(\psi_j)_{j \in \mathbb{Z}}$ where $\psi_j := 2^j \psi(2^j(\cdot))$ for a so-called mother wavelet $\psi: \mathbb{R} \rightarrow \mathbb{R}$. If we define $v_j := \psi_j$ for $j \geq 1$ and select v_0 such that $|\mathbf{F}_1 v_0|^2 = \sum_{j \leq 0} |\mathbf{F}_1 \psi_j|^2$ we obtain a multiscale decomposition $(u_j)_{j \in \mathbb{N}}$. Alternatively, for the low resolution filter we can take any other function v_0 such

that $|\mathbf{F}_1 v_0|^2 + \sum_{j \geq 1} |\mathbf{F}_d \psi_j|^2$ is bounded and away from zero by reasonable constants. Several examples of dyadic translation invariant wavelet frames can be extracted from classical wavelet analysis [8, 34]. Among many others, examples for the generating mother wavelet $\psi = v_0$ are Mexican hat wavelets, Shannon wavelets, spline wavelets or Meyer wavelets. For our numerical simulations, we use the Mexican hat wavelet.

4 Application to compressed sensing PAT

In this section, we extend the multiscale factorization to the case of compressed sensing data in PAT. Moreover, we derive a corresponding sparse recovery scheme.

4.1 Sampling the wave equation

When realizing a PAT setup, the acoustic data can only be collected for a finite number of sampling points that we denote by $z_\ell \in S$ for $\ell \in \{1, \dots, n\}$. Note that we do not discretize the temporal variable since temporal samples can easily be collected at rate well above the Nyquist sampling rate.

Definition 13 (Sampled PAT forward operator). Let \mathbf{W} be the continuous PAT forward operator defined in (5). For sampling points $z_\ell \in S$, $\ell \in \{1, \dots, n\}$, we set

$$\mathbf{S}_n: C^\infty(S \times (0, \infty)) \rightarrow (C^\infty(0, \infty))^n: g \mapsto (g(z_\ell, \cdot))_{\ell=1, \dots, n} \quad (22)$$

$$\mathbf{W}_n: C^\infty(\mathbb{R}^d) \rightarrow (C^\infty(0, \infty))^n: f \mapsto \mathbf{S}_n \mathbf{W} f = (p(z_\ell, \cdot))_{\ell=1, \dots, n}. \quad (23)$$

We call \mathbf{S}_n the regular sampling scheme and $\mathbf{W}_n = \mathbf{S}_n \mathbf{W}$ the (regularly) sampled PAT forward operator corresponding to the n -tuple $(z_\ell)_{\ell=1, \dots, n}$ of spatial sampling points.

The fundamental question of classical Shannon sampling theory in the context of PAT is finding “simple” sets \mathbb{X} where the initial pressure belongs to and associated conditions on the sampling points under which the sampled data $\mathbf{W}_n f$ uniquely determine the initial pressure distribution $f \in \mathbb{X}$. For equispaced detectors on the boundary of a disc $D \subseteq \mathbb{R}^2$, explicit sampling conditions for PAT have been derived in [22]. Roughly spoken, these results state that any function $f \in C_0^\infty(D)$ whose Fourier transform $\hat{f}(\xi)$ is sufficiently small for $\|\xi\| \geq b_0$, where b_0 is the bandwidth, can be stably recovered from sampled PAT data $\mathbf{W}_n f$ provided that the sampling condition $n \geq 2R_0 b_0$ is satisfied (for a precise statement see [22]). Sampling theory for other tomographic inverse problems is discussed, for example, in [43, 28, 13, 10, 36].

4.2 Compressive sampling

In order to reduce the number of detectors while preserving spatial resolution CSPAT has been studied in several works [19, 41, 4, 4, 19]. The basic idea is to use general linear measurements of the form

$$y_j = \langle a_j, \mathbf{W}_n(f) \rangle = \sum_{i=1}^n a_{j,i} (\mathbf{W}_n(f))_i \quad \text{for } j \in \{1, \dots, m\}. \quad (24)$$

Here a_j are measurement vectors with entries $a_{j,i}$ and $\mathbf{A}_{m,n} := (a_{j,i})_{j,i} \in \mathbb{R}^{m \times n}$ is the measurement matrix. The term compressed sensing refers to the fact that the number of measurements m is intended to be chosen much smaller than the number of initial sampling points n . Therefore $y = \mathbf{A}_{m,n} \mathbf{W}_n f$ constitutes a highly under determined system of linear equations and can only be solved with additional assumptions on unknown to be reconstructed.

For a systematic treatment, we introduce the following notation.

Definition 14 (Generalized sampling in PAT). For sampling points $(z_\ell)_{\ell=1,\dots,n} \in S^n$, measurement matrix $\mathbf{A}_{m,n} \in \mathbb{R}^{m \times n}$ and subspace $\mathbb{X} \subseteq C^\infty(\mathbb{R}^d)$ we call

- (a) $\mathbf{A}_{m,n} \mathbf{S}_n$ a generalized sampling scheme;
- (b) $\mathbf{A}_{m,n} \mathbf{W}_n = \mathbf{A}_{m,n} \mathbf{S}_n \mathbf{W}$ CSPAT forward operator;
- (c) $\mathbf{A}_{m,n} \mathbf{S}_n$ a complete sampling scheme for \mathbb{X} , if the restriction $\mathbf{A}_{m,n} \mathbf{S}_n \mathbf{W}|_{\mathbb{X}}$ is injective.

The results of [22] essentially show that \mathbf{S}_n gives a complete sampling scheme on the space $V = V_{R_0, b_0}$ of all functions being supported in a disc of radius R_0 and having essential bandwidth b_0 for $n \geq 2R_0 b_0$ equally distributed sampling points. This implies that for any invertible matrix $\mathbf{A}_{m,n}$, the composition $\mathbf{A}_{m,n} \mathbf{S}_n$ is a complete sampling scheme on V_{R_0, b_0} as well. We are not aware of any results (even for related inverse problems) when the generalized sampling scheme cannot be written in the form $\mathbf{B} \mathbf{S}_m$ with \mathbf{S}_m being a regular sampling scheme and $\mathbf{A}_{m,n} \in \mathbb{R}^{n \times n}$ being invertible. The question for which spaces such a general sampling matrix are complete sampling schemes seems an interesting direction of open research. Anyway, in this paper we investigate the case when $\mathbf{A}_{m,n} \mathbf{W}_n$ is not injective on the linear subspace \mathbb{X} and develop a nonlinear reconstruction approach based on ℓ^1 -minimization.

4.3 Multiscale reconstruction for CSPAT

Let $\mathbf{W}_n = \mathbf{S}_n \mathbf{W}$ be a regularly sampled discrete PAT forward operator with sampling points $(z_\ell)_{\ell=1,\dots,n} \in S^n$. We suppose that the regular sampling scheme \mathbf{S}_n is complete for a subspace

$$\mathbb{X}_n \subseteq \mathcal{B}_\Omega(\mathbb{R}^n) := \{f \in L^2(\mathbb{R}^n) \mid f \text{ is } \Omega\text{-bandlimited}\}. \quad (25)$$

Here $f \in L^2(\mathbb{R}^d)$ is called Ω -bandlimited if $\text{supp}(\mathbf{F}_d f)(\xi)$ vanishes for $\|\xi\| > \Omega$. Note that we have $\mathcal{B}_\Omega(\mathbb{R}^d) \subseteq C^\infty(\mathbb{R}^d) \cap L^2(\mathbb{R}^d)$. Moreover, let $\mathbf{A}_{m,n} \in \mathbb{R}^{m \times n}$ be a measurement matrix with $m < n$ such $\mathbf{A}_{m,n} \mathbf{S}_n$ is not complete on \mathbb{X}_n . This means that $\mathbf{A}_{m,n} \mathbf{W}_n$ is not injective on \mathbb{X}_n and therefore cannot be uniquely inverted. Our aim is to nevertheless to recover $f \in \mathbb{X}_n$ from data $y = \mathbf{A}_{m,n} \mathbf{W}_n f$ by using suitable prior information.

Below we describe how a multiscale factorization for the wave equation can be used to recover an initial pressure from CSPAT data. The main ingredient for our approach is that the factorizations of Theorems 10 and Corollary 11 for the full wave equation generalize to the compressed sensing setup. Here we only formulate such an extension of Corollary 11, because we use this version for the numerical implementation.

Proposition 15 (Multiscale CSPAT decomposition). *Let (u, v) be a multiscale factorization of \mathbf{W} . Then for all $f \in L^2(\mathbb{R}^d)$ the factors $f_j = u_j \otimes_x f$ satisfy*

$$\Phi \otimes_x f = \sum_{j \in \mathbb{N}} (\mathbf{R}^\# v_j) * f_j \quad (26)$$

$$(\mathbf{A}_{m,n} \mathbf{W}_n) f_j = v_j \otimes_t ((\mathbf{A}_{m,n} \mathbf{W}_n) f). \quad (27)$$

with $\Phi := \mathbf{F}_d^{-1} \left(\sum_{j \in \mathbb{N}} |\mathbf{F}_d u_j|^2 \right)$.

Proof. This follows from Corollary 11 by simply noting that $\mathbf{A}_{m,n} \mathbf{S}_n$ acts in the spatial variable and therefore commutes with the temporal convolution. \square

4.4 Proposed multiscale reconstruction

Consider the situation as described in Subsection 4.3. Based on the factorization of Corollary 15 we propose the following reconstruction scheme from CSPAT data:

Algorithm 16 (Recover initial pressure f from CSPAT data $\mathbf{A}_{m,n} \mathbf{W}_n f$).

- (S1) Solve equation (27) for f_j as described below.
- (S2) Evaluate the series on the right hand side of (26).
- (S3) Solve the deconvolution problem (26) for f .

Because the $(v_j)_{j \in \mathbb{N}}$ is a convolutional frame, $\mathbf{F}_d \Phi$ is bounded away from zero and therefore the deconvolution problem (26) in step (S3) is stably solvable. However, because $\mathbf{A}_{m,n} \mathbf{W}_n$ is non-injective, solving (27) in step (S1) requires prior information. The proposed procedure is described in following in Remark 17.

Remark 17 (Solution of step (S1)). Appropriate prior information is different for the low frequency factor f_0 and the high frequency factors f_j for $j \geq 1$. We therefore recover the low frequency factor and the high frequency factors differently.

- **LOW FREQUENCY FACTOR:** Assuming that v_0 has essential bandwidth in b_0 , then low frequency factor $f_0 = u_0 \otimes_x f$ also has essential bandwidth b_0 . This means that the Fourier transform $\mathbf{F}_d f_0(\xi)$ is sufficiently small for $\|\xi\| \geq b_0$. Therefore, classical sampling theory in the context of PAT [22] shows that m regular samples are sufficient to recover $f_0 = u_0 \otimes_x f$ as solution of

$$\min_{h \in \mathbb{X}_n} \|h\|_2 \quad \text{such that } \mathbf{A}_{m,n} \mathbf{W}_n h = y_0. \quad (28)$$

We use (28) when $\mathbf{A}_{m,n} \in \mathbb{R}^{m \times n}$ is either a subsampling matrix or random sensing matrix.

- **HIGH FREQUENCY FACTORS:** Assuming that the Fourier transform $\mathbf{F}_1 v(\omega)$ is negligible in a suitable sense when $|\omega|$ is outside the interval $[b_0, 2b_0]$, then the Fourier transforms are of high factors $\mathbf{F}_d u(\xi)$ are negligible outside the annulus $D_j := \{\xi \in \mathbb{R}^d \mid [2^{j-1}b_0 \leq \|\xi\| \leq 2^j b_0]\}$. However if we perform compressive sampling, $\mathbf{A}_{m,n} \mathbf{W}_n$ will not be injective on the space of all functions that are essentially supported in D_j and therefore (26) cannot be inverted uniquely without additional prior information. As we observe from Figure 2 the high frequency factors $f_0 = u_0 \otimes_x f$ are sparse in the spatial domain. Therefore in this paper we propose to use ℓ^1 -minimizing solutions

$$\min_{h \in \mathbb{X}_n} \|h\|_1 \quad \text{such that } \mathbf{A}_{m,n} \mathbf{W}_n h = y_j. \quad (29)$$

Here $\|h\|_1 := \sum_{i \in \mathbb{Z}^2} |h(i\pi/\Omega)|$ is the ℓ^1 -norm of h at the discrete samples $x_i = \pi/\Omega$ advised by Shannon's sampling theorem.

We can derive uniqueness of (29) from compressed sensing conditions. Here we make use of the [18] dealing with the reconstruction of individual elements, which in our context read as follows:

- There exists $\eta \in \mathbb{R}^m$ with $(\mathbf{A}_{m,n} \mathbf{W}_n)^* \eta \in \text{Sign}(u_j \otimes_x f)$
- $\forall i \in I_n \setminus \text{supp}(u_{0,j} \otimes_x f): |\langle e_n, (\mathbf{A}_{m,n} \mathbf{W}_n)^* \eta \rangle| < 1.$
- The restricted mapping $(\mathbf{A}_{m,n} \mathbf{W}_n)_{\text{supp}(x^\dagger)}$ is injective on \mathbb{X}_j .

A detailed error analysis for CSPAT with Algorithm 16 using (28) for the low resolution factor and (29) for the high resolution factors is an interesting line of future research and beyond the scope of this paper.

5 Numerical experiments

In this section, we present details on the implementation of the sparse reconstruction scheme from compressed sensing measurements presented in Section 4. In our numerical experiments, we consider the two dimensional case when the initial pressure is supported in the unit disc in \mathbb{R}^2 of radius 0.9 and measurements are taken the unit sphere \mathbb{S}^1 . This situation appears in PAT with integrating line detectors [5, 14].

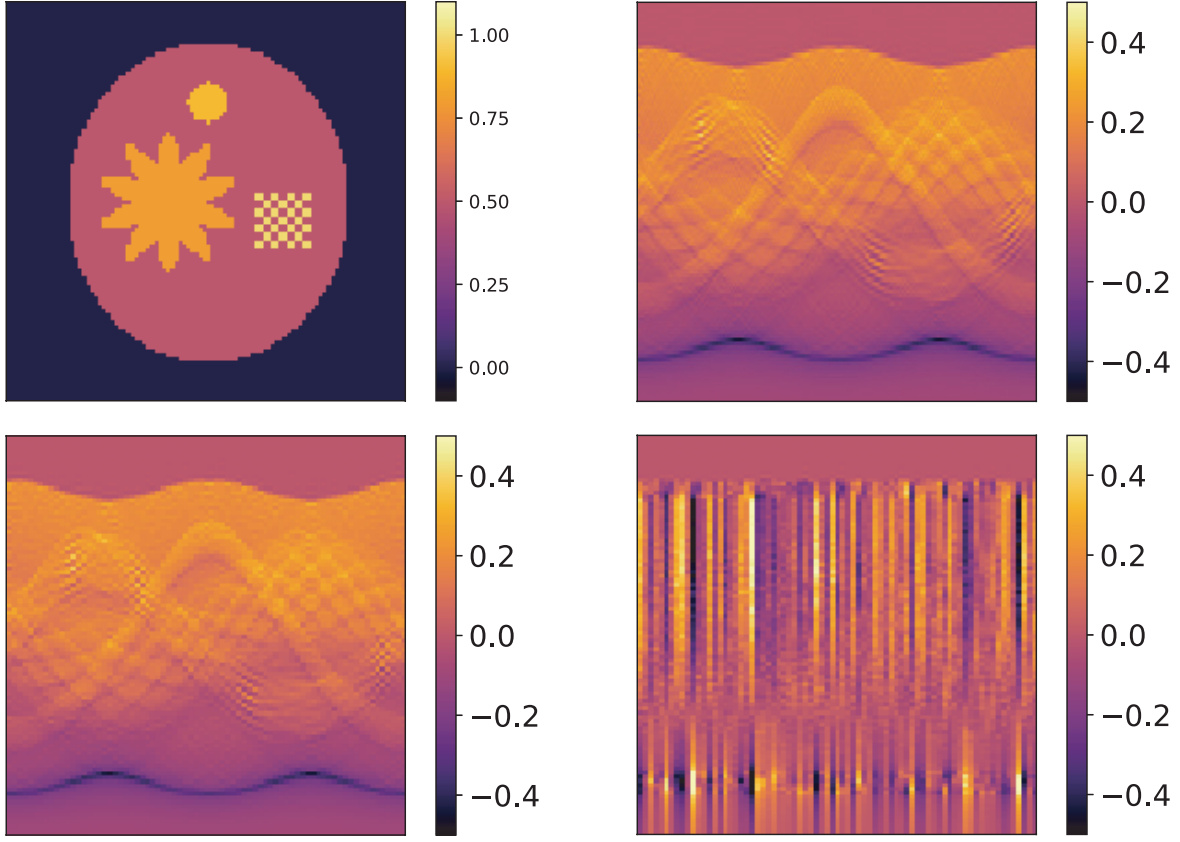


Figure 3: Left: Initial pressure on a square grid of side length 2. The point-like detectors are equidistantly distributed on the black circle. Right: Full data.

5.1 Numerical implementation

For all presented numerical implementations we replace f by its discrete values $(f(x_i))_i$ on a Cartesian grid of side length 2 at nodes $x_i = i 2/N_x$ for $i \in \{-N_x/2, \dots, N_x/2 - 1\}^2$ with $N_x = 100$. We assume that f is sampled at the Nyquist rate such that the maximal Bandwidth is given by $\Omega = N_x(\pi/2)$. The space \mathbb{X}_n in (25) is taken as the space of all $f \in \mathcal{B}_\Omega$ whose samples vanish outside the disc of radius 0.9. We implement \mathbf{W}_n and $\mathbf{A}_{m,n}$ with $n = 300$ and $m = 75$ as described below. Note that the fully sampled PAT forward operator \mathbf{W}_n satisfies the classical sampling conditions of [22]. The measurements matrix $\mathbf{A}_{m,n}$ corresponds to a subsampling factor of 4.

- **SAMPLED PAT FORWARD OPERATOR:** The discretization of \mathbf{W}_n is based on the Fourier representation $\mathbf{F}_d p(\xi, t) = \cos(\|\xi\| t) \mathbf{F}_d f(\xi)$ for the solution of the wave equation (2)-(4). For the numerically computation we replace the Fourier transform by the discrete Fourier transform on the square grid of side length 4 with spatial nodes $x_i = i 2/N_x$ for $i \in \{-N_x, \dots, N_x - 1\}^2$ and frequency nodes $\xi_k = k \Omega/N_x$ for $k \in \{-N_x, \dots, N_x - 1\}^2$. Here, the bandwidth Ω and the spatial sampling step size $2/N_x$ are satisfy the Nyquist condition $2/N_x = \pi/\Omega$ and the larger numerical domain is $[-2, 2] \times [-2, 2]$ is chosen to avoid boundary effects. We then define discrete fully sampled PAT forward operator \mathbf{W}_n by nearest neighbor interpolation at

the detector locations. The adjoint of \mathbf{W}_n^* is numerically computed via the backprojection algorithm described in [5].

- **MULTISCALE FILTERS:** The high frequency filters v_j for $j \geq 1$ are taken as Mexican hat wavelets

$$v_j(t) := 2^3 2^j (1 - (2^j 8t)^2) \exp\left(-\frac{(2^j 8t)^2}{2}\right)$$

and the corresponding low resolution temporal filter v_0 is taken as a Gaussian $v_0(t) := 2^3 \exp(-(8t)^2/2)$. The width of the filter v_0 is taken such that $v_0 \otimes_x f$ is can be recovered from $n = 75$ samples according to classical sampling theory. For the high frequency components $v_j \otimes_x f$ with $j \geq 1$ this is not the case, and therefore we use sparsity as described in Section (4). The spatial filters $u_j = \mathbf{R}^\# v_j$ are computed analytically by evaluating (8) for $d = 2$ and $v = v_j$. For $j \geq 2$, the essential support v_j lies outside the considered frequency regime $[-b, b]$ and therefore for the numerical simulations we use the three filters (v_0, v_1, v_2) . All temporal and spatial convolutions are replaced by discrete convolution via the discrete Fourier transform.

- **MEASUREMENT MATRIX:** For the measurement matrix $\mathbf{A}_{m,n} \in \mathbb{R}^{m \times n}$ we consider two choices. First, we take $\mathbf{A}_{m,n}$ as uniform subsampling matrix which has entries $a_{j,i} = 1$ if $j = 4(i-1)+1$ and $a_{j,i} = 0$ otherwise. Second we take $\mathbf{A}_{m,n}$ as Gaussian random matrix where each entry $a_{j,i}$ is the realization of an independent Gaussian random variables with zero mean.

The initial pressure used for the numerical simulations, the corresponding fully sampled data as well as the subsampled data and the Gaussian measurement data are shown in Figure 3. The filtered data for the subsampling scheme are shown in the left column of Figure 4 and the filtered data using Gaussian measurements in Figure 5.

5.2 Reconstruction results

Following the strategy proposed in Section 4 (see Algorithm 16 and Remark 17), we recover the initial phantom via the following three steps:

- First recover the factors $u_j \otimes_x f$ from data $y_j = v_j \otimes_x (\mathbf{A}_{m,n} \mathbf{W}_n f)$. For that purpose, we use the Landweber iteration for recovering the low frequency factor $u_0 \otimes_x f$ and the iterative soft thresholding algorithm

$$h_k = \text{soft}_{s\lambda} \left(h_k + s \mathbf{W}_n^* \mathbf{A}_{m,n}^* (\mathbf{T}_j f y - \mathbf{A}_{m,n} \mathbf{W}_n f_k) \right)$$

for recovering the sparse high frequency factors $u_1 \otimes_x f$ and $u_2 \otimes_x f$. Here $\text{soft}_{s\lambda} f = \text{sign}(f) \max\{|f| - s\lambda, 0\}$ is the soft thresholding operation, s the step size and λ the regularization parameter.

- Second we evaluate $f_{\text{conv}} := \sum_{j=0}^2 u_j \otimes_x f_j$.

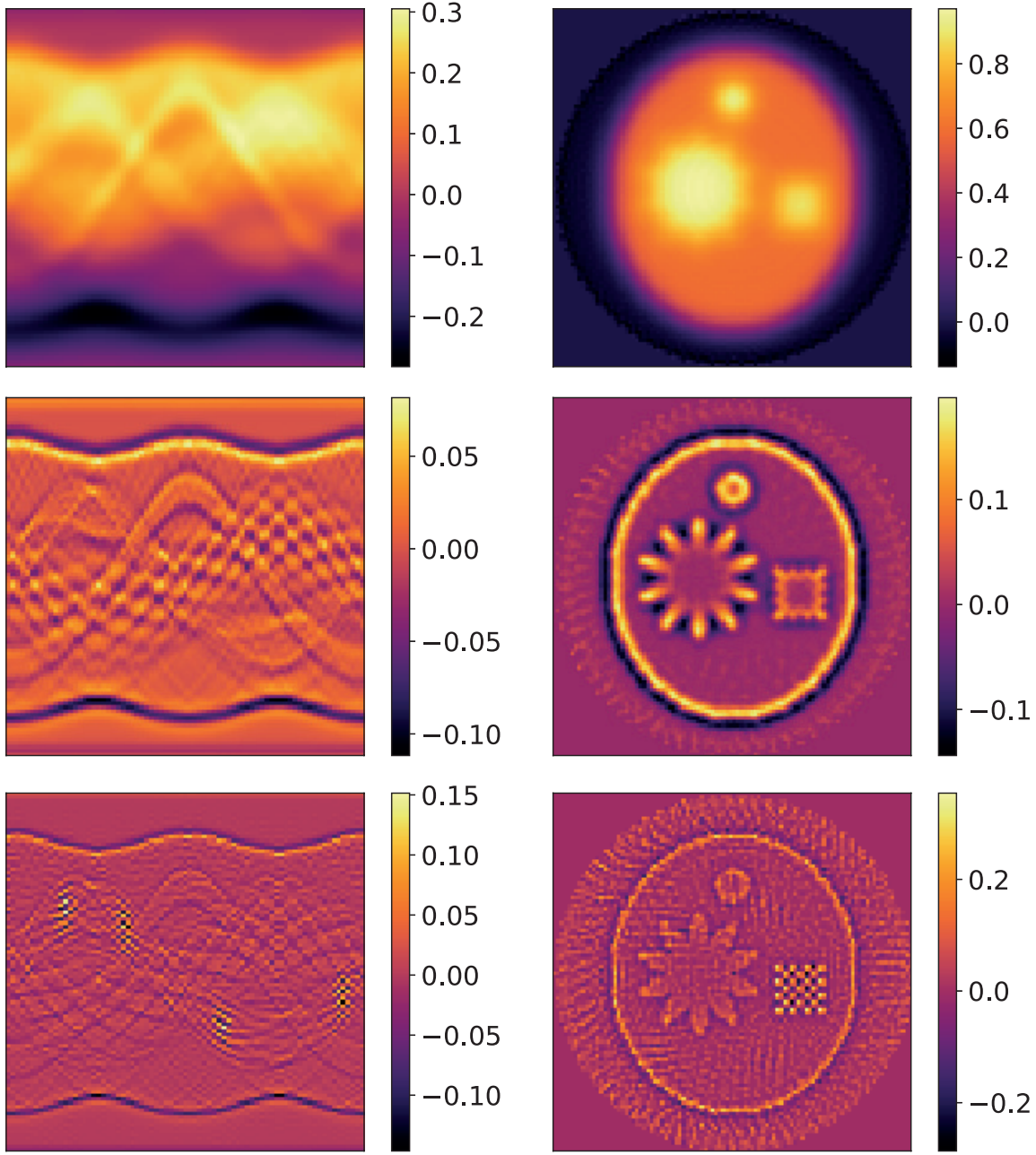


Figure 4: Left: The convolved data $y_j = v_j \otimes_t (\mathbf{A}_{m,n} \mathbf{W}_n f)$ for $j = 0, 1, 2$ where $\mathbf{A}_{m,n}$ is the subsampling matrix with subsampling factor 4. Right. Corresponding reconstructions of convolved initial pressure $u_j \otimes_x f$ using the Landweber method (for $j = 0$) and iterative soft thresholding (for $j = 1, 2$).

- As a final reconstruction step we recover an approximation to f by deconvolution f_{conv} with kernel $\Phi = \mathbf{F}_d^{-1} \sum_{j=0}^2 |\mathbf{F}_d u_j|^2$. In this work we again use the iterative soft thresholding algorithm for performing the deconvolution.

The reconstructions of the convolved phantoms for the subsampling measurements are shown in the right column in Figure 4 and the for the Gaussian measurements in the right column in Figure 5.

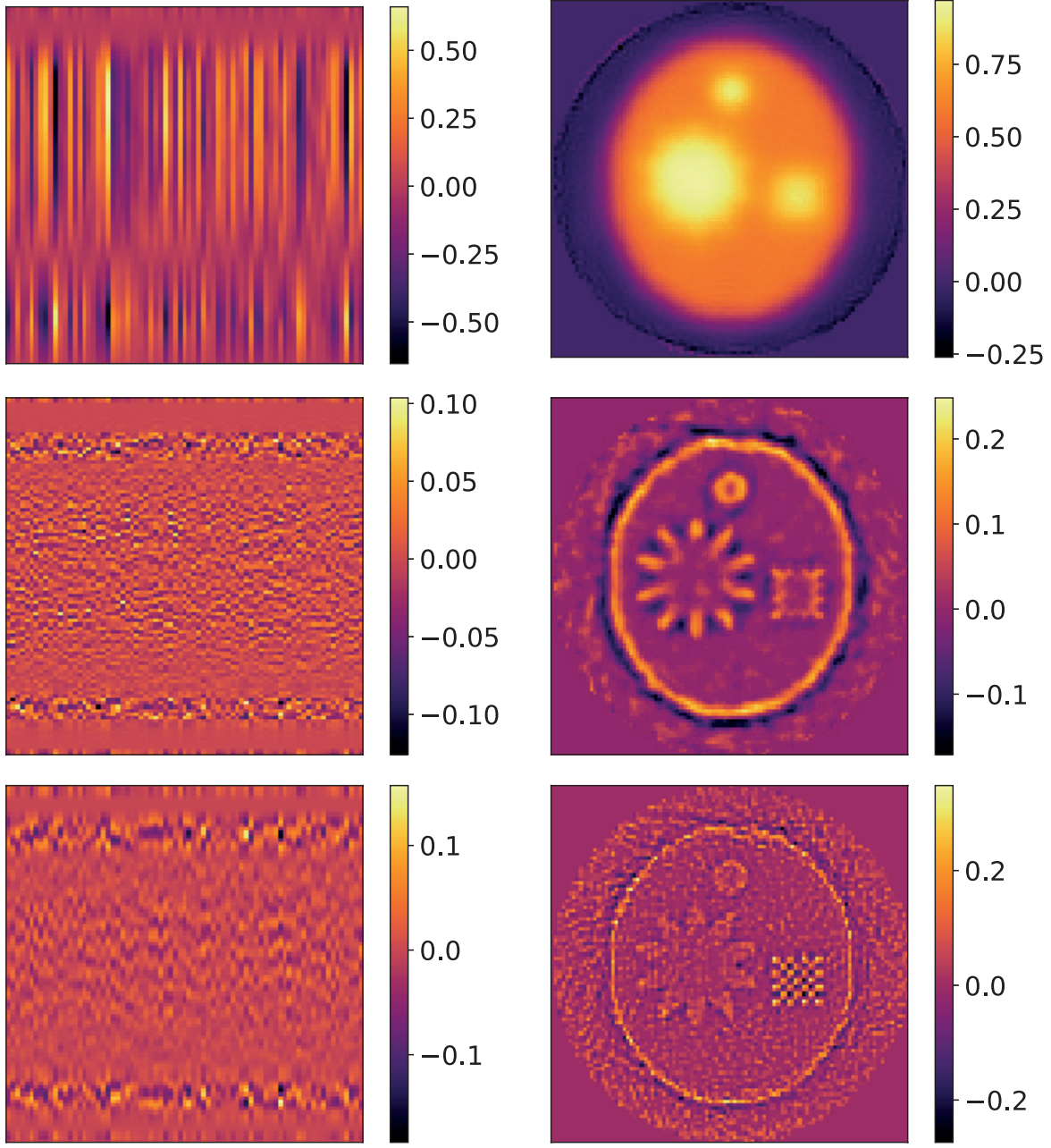


Figure 5: Left: The convolved data $y_j = v_j \otimes_t (\mathbf{A}_{m,n} \mathbf{W}_n f)$ for $j = 0, 1, 2$ where $\mathbf{A}_{m,n}$ is a Gaussian random matrix with subsampling factor 4. Right: Corresponding reconstructions of convolved initial pressure $u_j \otimes_x f$ using the Landweber method (for $j = 0$) and iterative soft thresholding (for $j = 1, 2$).

The right column in Figure 6 shows the resulting reconstructions from subsampled measurements and Gaussian measurements. The left column shows the reconstructions using standard ℓ^1 -minimization without out multiscale sparsifying transforms. The relative ℓ^2 -reconstruction errors are 0.17 (sparse sampling) and 0.19 (Gaussian measurements) for the proposed method and 0.22 (both cases) for standard ℓ^1 -minimization with iterative soft thresholding. Notably, the high-resolution pattern is reconstructed significantly better for the proposed multiscale approach that

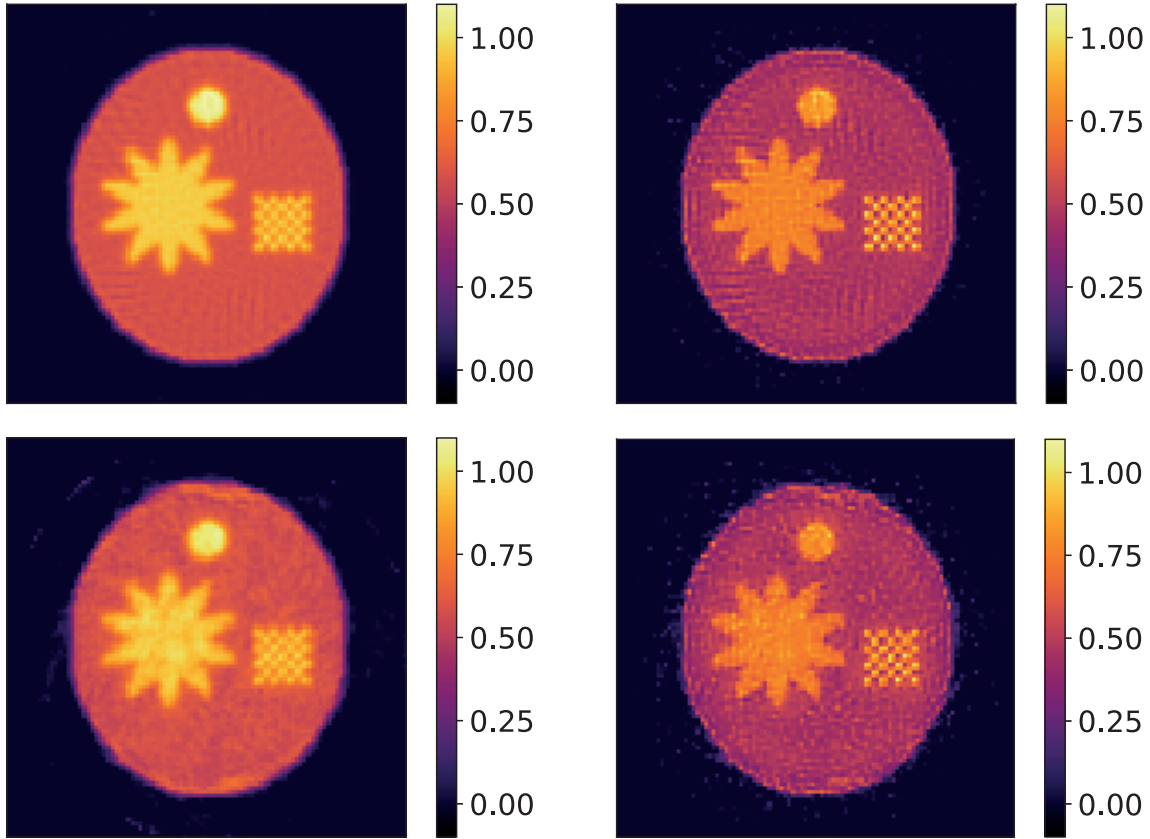


Figure 6: Top: Reconstruction from sparse measurements $y = \mathbf{A}_{m,n} \mathbf{W}_n f$ with subsampling factor 4 using standard ℓ^1 -minimization (left) and the proposed algorithm (right). Bottom: Same for Gaussian measurements.

for standard ℓ^1 -minimization.

6 Conclusion

In this paper, we derived a multiscale factorization of the wave equation. We applied the multiscale factorization to CSPAT, where reconstructions are obtained from only a few compressed sensing measurements that consist of linear combinations of the signals recorded by individual point-like detectors. We present a novel multiscale reconstruction approach that uses the acoustic reciprocal principle to achieve a multiscale decomposition of the desired initial pressure by applying a family of operators that act on acoustic data in the time domain. In this way sparsity of the desired initial pressure distribution can be introduced for the high scales of the operators. Our numerical results demonstrate that the proposed method improves the reconstructions in the case of compressed sensing measurements.

In future work, we will improve and analyze the reconstruction algorithm associated to the multiscale factorization. In particular, we analyze the theoretical conditions for unique recovery. Other interesting lines of future research is the extension of the proposed method to PAT with variable

sound speed as well as other tomographic image reconstruction modalities. During finalization of the manuscript we found that in the context of Radon inversion with filtered backprojection, related multiscale factorizations have been proposed in [39, 7]. The combination of such results with compressed sensing and more advanced reconstruction techniques seems an interesting line of research.

Acknowledgments

This work has been supported by the Austrian Science Fund (FWF), project P 30747-N32.

A Proof of Proposition 2

According to Proposition 1 it is sufficient to show that $\mathbf{R}^\# v$ is a solution of the equation $v = \mathbf{R} u$. Recalling the definition of \mathbf{R} in (6) this amounts in showing that $\mathbf{R}^\# v = \bar{u} \circ \|\cdot\|$ satisfies the integral equation $v(t) = \omega_{d-2} \int_{|t|}^\infty s \bar{u}(s) (s^2 - t^2)^{(d-3)/2} ds$ for $t \in \mathbb{R}$. We note that $(\theta, t) \mapsto \mathbf{R} u(t)$ is the Radon transform of the radially symmetric function u . Therefore, there is exactly one radial function satisfying the above integral equation. An explicit expression for the solution has been given in [9]. Using elementary computation, a formula has been derived in [35, p. 23]. By slight modification we obtain the following results.

Lemma 18. *The solution $u = \bar{u} \circ \|\cdot\|$ of the equation $v = \mathbf{R} u$ is given by*

$$\forall r > 0: \quad \bar{u}(r) := \frac{2(-1)^{d-1}}{\pi^{(d-1)/2} \Gamma((d-1)/2)} \mathbf{D}_r^{d-1} \int_r^\infty (t^2 - r^2)^{(d-3)/2} v(t) t dt. \quad (30)$$

Proof. In [35, p. 23] the identity $\mathbf{D}_r^{d-1} \int_r^\infty (t^2 - r^2)^{(d-3)/2} v(t) t dt = 2^{-1} (-1)^{d-1} \omega_{d-2} c(d) (d-2)! \bar{u}(r)$ has been derived with $c(d) := 2^{1-d} \int_{-1}^1 (1 - s^2)^{(d-3)/2} ds$. Together with the identities $\omega_{d-2} = 2\pi^{(d-1)/2} / \Gamma((d-1)/2)$ and $c(d) = 2^{1-d} \pi^{1/2} \Gamma((d-1)/2) / \Gamma(d/2)$ as well as $\Gamma(d/2) \Gamma((d-1)/2) = 2^{2-d} \pi^{1/2} (d-2)!$ imply the explicit solution formula (30). \square

It remains to bring the right hand side of Equation (30) in the desired form. We do this separately for the even and odd dimensional case.

■ If d is odd we have

$$\begin{aligned} & \mathbf{D}_r^{(d-1)/2} \mathbf{D}_r \mathbf{D}_r^{(d-3)/2} \int_r^\infty (t^2 - r^2)^{(d-3)/2} v(t) t dt \\ &= (-1)^{(d-3)/2} ((d-3)/2)! \mathbf{D}_r^{(d-1)/2} \mathbf{D}_r \int_r^\infty v(t) t dt \\ &= (-1)^{(d-1)/2} \frac{((d-3)/2)!}{2} \mathbf{D}_r^{(d-1)/2} v(r). \end{aligned}$$

Together with Lemma 18 this gives (8) for d odd.

■ If d is even we first compute

$$\begin{aligned}
& \mathbf{D}_r \int_r^\infty \frac{v(t)}{\sqrt{t^2 - r^2}} t dt \\
&= \mathbf{D}_r \int_r^\infty \left(\partial_t \sqrt{t^2 - r^2} \right) \phi(t) dt \\
&= - \mathbf{D}_r \int_r^\infty \sqrt{t^2 - r^2} \left(\partial_t \phi(t) \right) dt \\
&= \int_r^\infty \frac{1}{2} \frac{1}{\sqrt{t^2 - r^2}} (\partial_s \phi(t)) dt \\
&= \int_r^\infty \frac{\mathbf{D}_t \phi(t)}{\sqrt{t^2 - r^2}} t dt.
\end{aligned} \tag{31}$$

Therefore

$$\begin{aligned}
& \mathbf{D}_r^{d/2} \mathbf{D}_r^{(d-2)/2} \int_r^\infty (t^2 - r^2)^{(d-3)/2} v(t) t dt \\
&= (-1)^{(d-2)/2} \Gamma((d-1)/2) \mathbf{D}_r^{d/2} \int_r^\infty (t^2 - r^2)^{-1/2} v(t) t dt \\
&= (-1)^{(d-2)/2} \Gamma((d-1)/2) \int_r^\infty \frac{\left(\frac{1}{2t} \frac{\partial}{\partial t} \right)^{d/2} v(t)}{\sqrt{t^2 - r^2}} t dt,
\end{aligned}$$

where the last equality follows after $(d/2)$ -times applying equality (31). This gives (8) for d even.

References

- [1] S. ACOSTA AND C. MONTALTO, *Multiwave imaging in an enclosure with variable wave speed*, Inverse Probl., 31 (2015), p. 065009.
- [2] M. AGRANOVSKY AND P. KUCHMENT, *Uniqueness of reconstruction and an inversion procedure for thermoacoustic and photoacoustic tomography with variable sound speed*, Inverse Probl., 23 (2007), p. 2089.
- [3] H. AMMARI, E. BRETIN, J. GARNIER, AND A. WAHAB, *Time reversal in attenuating acoustic media*, Contemporary Mathematics, 548 (2011), pp. 151–163.
- [4] S. ARRIDGE, P. BEARD, ET AL., *Accelerated high-resolution photoacoustic tomography via compressed sensing*, Phys. Med. Biol., 61 (2016), pp. 8908–8940.
- [5] P. BURGHOLZER, J. BAUER-MARSHALLINGER, ET AL., *Temporal back-projection algorithms for photoacoustic tomography with integrating line detectors*, Inverse Probl., 23 (2007), p. S65.

- [6] E. J. CANDÈS, J. K. ROMBERG, AND T. TAO, *Stable signal recovery from incomplete and inaccurate measurements*, Comm. Pur. Appl. Math., 59 (2006), pp. 1207–1223.
- [7] M. COSTIN, D. LAZARO-PONTHUS, ET AL., *A 2D multiresolution image reconstruction method in x-ray computed tomography*, J. X-ray Sci. Technol., 19 (2011), pp. 229–247.
- [8] I. DAUBECHIES, *Ten lectures on wavelets*, vol. 61, Siam, 1992.
- [9] S. DEANS, *Gegenbauer transforms via the Radontransform*, SIAM J. Math. Anal., 10 (1979), pp. 577–585.
- [10] L. DESBAT, *Efficient sampling on coarse grids in tomography*, Inverse Probl., 9 (1993), p. 251.
- [11] D. L. DONOHO, *Compressed sensing*, IEEE Trans. Inf. Theory, 52 (2006), pp. 1289–1306.
- [12] F. DREIER AND M. HALTMEIER, *Explicit inversion formulas for the two-dimensional wave equation from neumann traces*, SIAM J. Imaging Sci., 13 (2020), pp. 589–608.
- [13] A. FARIDANI, *Fan-beam tomography and sampling theory*, in The Radon transform, inverse problems, and tomography, vol. 63, AMS, 2006, pp. 43–66.
- [14] D. FINCH, *The spherical mean value operator with centers on a sphere*, Inverse Probl., 23 (2007), p. S37.
- [15] D. FINCH, M. HALTMEIER, AND RAKESH, *Inversion of spherical means and the wave equation in even dimensions*, SIAM J. Appl. Math., 68 (2007), pp. 392–412.
- [16] D. FINCH, S. K. PATCH, AND RAKESH, *Determining a function from its mean values over a family of spheres*, SIAM J. Math. Anal., 35 (2004), pp. 1213–1240.
- [17] S. FOUCART AND H. RAUHUT, *A mathematical introduction to compressive sensing*, Bull. Am. Math, 54 (2017), pp. 151–165.
- [18] M. GRASMAIR, O. SCHERZER, AND M. HALTMEIER, *Necessary and sufficient conditions for linear convergence of ℓ^1 -regularization*, Comm. Pure Appl. Math., 64 (2011), pp. 161–182.
- [19] Z. GUO, C. LI, L. SONG, AND L. V. WANG, *Compressed sensing in photoacoustic tomography in vivo*, J. Biomed. Opt., 15 (2010), p. 021311.
- [20] M. HALTMEIER, *A mollification approach for inverting the spherical mean Radon transform*, SIAM J. Appl. Math., 71 (2011), pp. 1637–1652.
- [21] M. HALTMEIER, *Universal inversion formulas for recovering a function from spherical means*, SIAM J. Math. Anal., 46 (2014), pp. 214–232.
- [22] M. HALTMEIER, *Sampling conditions for the circular Radon transform*, IEEE Trans. Image Process., 25 (2016), pp. 2910–2919.

- [23] M. HALTMEIER, T. BERER, S. MOON, AND P. BURGHOLZER, *Compressed sensing and sparsity in photoacoustic tomography*, J. Opt., 18 (2016), p. 114004.
- [24] M. HALTMEIER AND . NGUYEN, *Analysis of iterative methods in photoacoustic tomography with variable sound speed*, SIAM J. Imaging Sci., 10 (2017), pp. 751–781.
- [25] M. HALTMEIER, M. SANDBICHLER, ET AL., *A sparsification and reconstruction strategy for compressed sensing photoacoustic tomography*, J. Acoust. Soc. Am., 143 (2018), pp. 3838–3848.
- [26] M. HALTMEIER AND G. ZANGERL, *Spatial resolution in photoacoustic tomography: effects of detector size and detector bandwidth*, Inverse Probl., 26 (2010), p. 125002.
- [27] C. HUANG, K. WANG, L. NIE, AND M. A. WANG, L. V. AND ANASTASIO, *Full-wave iterative image reconstruction in photoacoustic tomography with acoustically inhomogeneous media*, IEEE Trans. Med. Imag., 32 (2013), pp. 1097–1110.
- [28] A. KATSEVICH, *A local approach to resolution analysis of image reconstruction in tomography*, SIAM J. Appl. Math., 77 (2017), pp. 1706–1732.
- [29] R. KOWAR, *On time reversal in photoacoustic tomography for tissue similar to water*, SIAM J. Imaging Sci., 7 (2014), pp. 509–527.
- [30] R. KOWAR AND O. SCHERZER, *Photoacoustic imaging taking into account attenuation*, in Mathematics and Algorithms in Tomography, vol. 18, Springer, 2012, pp. 54–56.
- [31] P. KUCHMENT AND L. KUNYANSKY, *Mathematics of thermoacoustic tomography*, Eur. J. Appl. Math., 19 (2008), pp. 191–224.
- [32] L. KUNYANSKY, *Reconstruction of a function from its spherical (circular) means with the centers lying on the surface of certain polygons and polyhedra*, Inverse Probl., 27 (2011), p. 025012.
- [33] L. KUNYANSKY, *Inversion of the spherical means transform in corner-like domains by reduction to the classical Radon transform*, Inverse Probl., 31 (2015), p. 095001.
- [34] S. MALLAT, *A wavelet tour of signal processing: The sparse way*, Elsevier/Academic Press, Amsterdam, third ed., 2009.
- [35] F. NATTERER, *Computerized tomography*, in The Mathematics of Computerized Tomography, Springer, 1986, pp. 1–8.
- [36] F. NATTERER, *Sampling and resolution in CT*, in Computerized tomography (Novosibirsk, 1993), VSP, Utrecht, 1995, pp. 343–354.
- [37] L. V. NGUYEN, *A family of inversion formulas for thermoacoustic tomography*, Inverse Probl., 3 (2009), pp. 649–675.
- [38] R. NUSTER, G. ZANGERL, M. HALTMEIER, AND G. PALTAUF, *Full field detection in photoacoustic tomography*, Opt. Express, 18 (2010), pp. 6288–6299.

- [39] F. PEYRIN, M. ZAIM, AND R. GOUTTE, *Multiscale reconstruction of tomographic images*, in Proc. IEEE Int. Symp. on Time-Frequency and Time-Scale Analysis, 1992, pp. 219–222.
- [40] J. POUDEL, Y. LOU, AND M. A. ANASTASIO, *A survey of computational frameworks for solving the acoustic inverse problem in three-dimensional photoacoustic computed tomography*, Phys. Med. Biol., 64 (2019), p. 14TR01.
- [41] J. PROVOST AND F. LESAGE, *The application of compressed sensing for photo-acoustic tomography*, IEEE Trans. Med. Imag., 28 (2009), pp. 585–594.
- [42] M. SANDBICHLER, F. KRAHMER, ET AL., *A novel compressed sensing scheme for photoacoustic tomography*, SIAM J. Appl. Math., 75 (2015), pp. 2475–2494.
- [43] P. STEFANOV, *Semiclassical sampling and discretization of certain linear inverse problems*, arXiv:1811.01240, (2018).
- [44] P. STEFANOV AND G. UHLMANN, *Thermoacoustic tomography with variable sound speed*, Inverse Probl., 25 (2009), p. 075011.
- [45] M. XU AND L. V. WANG, *Photoacoustic imaging in biomedicine*, Rev. Sci. Instrum., 77 (2006), p. 041101.
- [46] G. ZANGERL, O. SCHERZER, AND M. HALTMEIER, *Exact series reconstruction in photoacoustic tomography with circular integrating detectors*, Commun. Math. Sci., 7 (2009), pp. 665–678.